

RESEARCH ARTICLE

Microwave Reflectometry Sensing System for Low-Cost in-vivo Skin Cancer Diagnostics

RAISSA SCHIAVONI¹, GENNARO MAIETTA², ELISABETTA FILIERI², ANTONIO MASCIULLO¹, AND ANDREA CATALDO¹, (Senior Member, IEEE)

¹Department of Engineering for Innovation, University of Salento, 73100 Lecce, Italy

²Local Health Unit of Lecce, 73100 Lecce, Italy

Corresponding author: Andrea Cataldo (andrea.cataldo@unisalento.it)

This work involved human subjects or animals in its research. Approval of all ethical and experimental procedures and protocols was granted by the Ethical Committee of Local Unit of Lecce (ASL LECCE).

ABSTRACT Skin cancer is one of the most commonly diffused cancers in the world and its incidence rates have constantly increased in recent years. At the current state of the art, there is a lack of objective, quick and non-invasive methods for diagnosing this condition; this, combined with hospital crowding, may lead to late diagnosis. Starting from these considerations, this paper addresses the implementation of a microwave reflectometry based-system that can be used as a non-invasive method for the in-vivo diagnosis and early detection of biological abnormalities, such as skin cancer. This system relies on the dielectric contrasts existing between normal and anomalous skin tissues at microwave frequencies (in a frequency range up to 3 GHz). In particular, a truncated open-ended coaxial probe was designed, manufactured and tested to sense (in combination with a miniaturized Vector Network Analyzer) the variations of skin dielectric properties in a group of volunteer patients. The specific data processing demonstrated the suitability of the system for discriminating malignant and benign lesions from healthy skin, ensuring simultaneously effectiveness, low cost, compactness, comfortability, and high sensitivity.

INDEX TERMS Cancer diagnostics, dielectric permittivity, frequency-domain measurements, in-vivo measurements, microwave reflectometry, open ended coaxial probe, PCA, skin abnormalities, skin cancer.

I. INTRODUCTION

The Skin Cancer Foundation estimates that in the U.S., more than 9.500 people are diagnosed with skin cancer every day and more than two people die of the disease every hour, according to data collected in the year 2022 [1]. Skin cancer, in fact, is the most common type of cancer and a large number of tumour types can affect the skin, which is the human body's largest organ [2]. The most common skin cancers, apart from melanoma, are basal cell carcinoma (BCC) [3], [4], [5], squamous cell carcinoma (SCC) [6], [7] and epithelioma. An early diagnosis is the key to guarantee the possibility of full recovery and to prevent the tumour from penetrating further into the underlying tissues causing

metastasis. However, currently, there is a lack of objective non-invasive methods for the characterization of skin lesions and the related diagnosis, that can ensure simultaneously an in-vivo modality, large-use possibility and low-cost instrumentation. As a matter of fact, when some suspicious cases occur, typically, the dermatologist performs a visual examination of the skin through epiluminescence [8]. Although the subjective expert diagnosis of the medical personnel remains the main clinical assessment, the proposed system is not intended to replace the dermatologist's opinion, instead, it can be a useful tool to improve diagnostic accuracy and to support the doctor in making a more objective diagnosis. In this regard, it is also worth noting that the possibility to have an additional diagnostic tool operating in-vivo, which is easy to use and transport and with a very quick response time, can significantly enhance the operational aspects of the clinical

The associate editor coordinating the review of this manuscript and approving it for publication was Wenbing Zhao¹.

procedure including the possibility to optimize the requests of biopsies. In fact, a definite diagnosis of cancer can be made only after a biopsy [9], [10], which is an invasive procedure involving the removal of a portion of tissue and, consequently, the analysis with a microscope. Because of the high error probability deriving from the dermatologist exams, biopsies are requested very frequently, even for portions of the skin that are actually healthy, causing discomfort and concern to the patients. On such basis, it goes without saying that, in the perspective of the so-called Health 4.0 Era [11], [12], the development of advanced digital technologies, new systems and wearable devices play a crucial role in improving health-care through periodical screening, diagnosis and treatment of cancers. For these purposes, a microwave reflectometry-based system was developed for analysing in-vivo suspicious skin lesions. The proposed methodology is based on the detection of the dielectric contrast between healthy and anomalous skin tissues at microwaves. As detailed in the following, a truncated open-ended coaxial probe [13], [14], [15], [16], [17] was designed, manufactured and tested to sense (in combination with a miniaturized Vector Network Analyzer) the variations of skin dielectric properties on a group of volunteer patients. The proposed sensing system has the twofold purpose of i) detecting early-stage cancer; and of ii) monitoring the healing phase and the evolution in time of cutaneous areas which were subjected to surgeries after cancers with periodic control.

This paper is organized as follows. First, Section II addresses the motivations of the work and provides an overview of state-of-the-art solutions for monitoring and diagnosis of skin cancers. Section III describes the basic theoretical background behind the proposed system. Section IV presents the design, the optimization and the characterization of the non-invasive coaxial probe. Section V describes the experimental measurement setup, the procedure for extrapolating the dielectric properties of skin tissues from the reflectometric measurements and the investigative campaign on people and voluntary patients. Section VI reports the experimental results together with the statistical analysis performed on the data. Finally, conclusions and future work are outlined in Section VII.

II. REVIEW OF THE STATE OF THE ART AND MOTIVATION OF THE PRESENT WORK

As briefly discussed in Section I, in the literature, most works relate to different methodologies for skin cancer detection, ranging from photodynamic, sonography, thermal imaging, optical electromagnetic microscopic imaging and electromagnetic techniques based on the extrapolation of dielectric properties of tissues. More in detail, confocal Raman spectroscopy [18] performs the analysis of the light that is scattered by the tissue; this, however, requires very costly instrumentation [19]. Similarly, methods such as near-IR [20] or Terahertz spectroscopy [21], [22] involve expensive equipment. Other technologies such as Bio-electrical

impedance or Optical Coherence Tomography (OCT) [23] may be affected by low measurement accuracy and they are both significantly influenced by physiological or environmental variations. Considering the aforementioned limitations, the proposed system exploits microwave reflectometry, combining the requirements of (i) low cost, (ii) compactness, (iii) quick response time, (iv) comfortability (no biopsy) and (v) high sensitivity. More specifically, this technique is particularly sensitive to the different dielectric properties between normal skin and lesions. As a matter of fact, cancer tissue differs in composition with respect to healthy tissue from which cancer originated [24]. Some of the factors that contribute to these variations include increased vasculature and blood content [25], differences in protein and mineral content [26] as well as differences in the water content or water distribution and structure, e.g., whether the water is free or bound. This means that it is extremely important to perform in-vivo diagnostics, in order to preserve the physical and chemical composition of suspect tissues. In fact, it is important to underline that, when excised, the tissues under test present some differences in characteristics with respect to the original in-vivo status, due to different conditions such as the temperature, the loss of tissue water content after excision and the absence of blood circulation. In this regard, an additional applicative limitation of most of the state-of-the-art techniques related to the necessity of analysing of portions of tissues excised through biopsies [27], [28], [29], thus altering the intrinsic properties of the tissues. As a consequence, the final results on the discrimination of skin cancers are ambiguous and some substantial discrepancies are also observed among the data presented in different publications. These limitations motivate the development of systems capable of discriminating, directly in vivo [30], the significant dielectric variations of skin tissues associable to suspicious or malignant tumour cases at their very early stage, by comparing their dielectric response with reference healthy areas. Another limitation of the methods based on dielectric detection existing at the current state of the art relies on the analysis usually conducted at a single frequency [30], while permittivity of biological tissues depends strongly on the frequency. Moreover, as further consideration, operating in a lower frequency range implies significant advantages in terms of reduced costs and portability of equipment. Another aspect motivating the present work relates to the possibility of diagnosing tumours at their earliest stage. In fact, if not diagnosed promptly, skin cancers can grow into nearby areas and they can invade and slowly destroy the surrounding tissues, as illustrated in Figure 1, provoking serious consequences that ultimately can lead to death.

In addition, knowing the dielectric signature of a body's portion can be critically important for several aspects beyond cancer diagnostics. It is worth noting that even when the treatment of carcinoma was successfully terminated, there is a residual possibility of a recurrence [32]. In the perspective of prevention measures, there is a need to monitor the dielectric variations of the skin area at risk in order to detect

TABLE 1. Dielectric parameters of 4-Cole&Cole model of [31].

Tissue	ϵ_∞	$\Delta\epsilon_1$	$\tau_1 [ps]$	α_1	$\Delta\epsilon_2$	$\tau_2 [ns]$	α_2	σ	$\Delta\epsilon_3$	$\tau_3 [\mu s]$	α_3	$\Delta\epsilon_4$	$\tau_4 [ms]$	α_4
Skin	4.00	32.00	7.23	0.00	1100	32.48	0.20	0.00	0.00	159.15	0.20	0.00	15.91	0.20
Fat	2.50	3.00	7.96	0.20	15.00	15.91	0.10	0.01	3.30E+4	159.15	0.05	1.00E+7	7.96	0.01
Muscle	4.00	50.00	7.23	0.10	7000	353.68	0.10	0.20	1.20E+6	318.31	0.10	2.50E+7	2.27	0.00

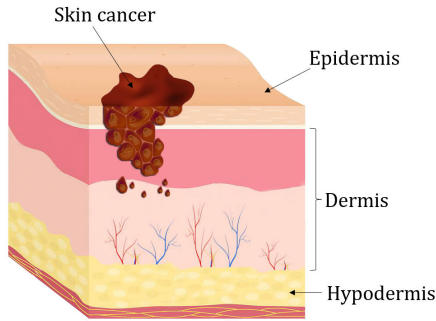


FIGURE 1. Growth of a skin cancer.

abnormalities in time. Viable tools for large-scale prevention monitoring could be useful also for several people such as workers frequently exposed to the sun [33] as well as others with risk factors including genetic predisposition [34], [35], [36], age [37], light skin, hair, and eye pigmentation [38], geographic position [39], [40], [41], fragile immune system [42], exposure to other radiation or to certain chemicals, chronic inflammatory skin conditions and complications of burns, scarring, or infections [43], [44]. On the basis of all the aforementioned aspects, the present work aims at proposing an alternative system that can detect suspicious or anomalous lesions directly in vivo and, at the same time, in the perspective of prevention. For the sake of assessing the proposed method, in this paper, investigations were conducted on some voluntary patients presenting different kinds of skin lesions which were preliminarily diagnosed by the standard so-called ABCDE visual analysis [45], [46].

III. THEORETICAL BACKGROUND

Microwave reflectometry (MR) is a powerful tool for several monitoring and diagnostic applications [47], [48], [49], [50], [51], [52], [53], [54], [55], [56], [57], [58], [59], [60]. Typically, in MR, an electromagnetic (EM) test signal is propagated through a sensing element. As a result of the electromagnetic interaction, the incident signal is reflected back and it carries significant information directly associable with the dielectric properties of the system under test. Because microwaves are non-ionizing radiation, they are suitable for diagnostic in-vivo applications on biological tissues, such as in the case of early-stage detection of skin cancer. As reported in the state of the art, the dielectric properties of cancer tissue differ from healthy tissue, mostly because of the different water and protein content [20], [61], [62]. This difference can be detected by microwave-based systems.

More specifically, the dielectric properties of biological tissues can be described in terms of frequency-dependent complex dielectric permittivity $\epsilon^*(f)$, according to the following equation 1

$$\epsilon^*(f) = \epsilon'(f) - j\epsilon''(f) \tag{1}$$

where ϵ' is the relative dielectric constant, ϵ'' is the relative dielectric loss factor and f is the frequency [63]. In this study, the considered frequency-dependent dielectric parameters of biological tissues have been adopted as reference by the ‘‘Gabriel&Gabriel’’ database. In particular, a four-terms Cole-Cole [31] expression is used, according to equation 2:

$$\epsilon^*(\omega) = \epsilon_\infty + \sum_{m=1}^4 \frac{\Delta\epsilon_m}{1 + (j\omega\tau_m)^{1-\alpha_m}} + \frac{\sigma}{j\omega\epsilon_0} \tag{2}$$

where ϵ_0 is the permittivity of free space equal to 8.85×10^{-12} F/m, ω is the angular frequency, σ is the conductivity, $j = \sqrt{-1}$ is the imaginary unit, $\Delta\epsilon$ and ϵ_∞ are the ‘‘static’’ and ‘‘infinite frequency’’ dielectric constants, and τ indicates the relaxation time. On such basis, this expression has been adopted as the most reliable fitting model in describing the dielectric properties of tissues and, consequently, to optimize the full-wave simulation results. In addition, Table 1 shows the parameters used to model each tissue layer. In particular, the dielectric contrast between cancerous and healthy tissues provokes a different interaction with microwaves, causing a reflected signal with different characteristics. The appropriate analysis of such a signal allows the differentiation between healthy and cancerous tissues. In fact, the dielectric characteristic is directly associated to the reflected signal, which can be revealed in terms of the frequency-dependent reflection scattering parameter $S_{11}(f)$ of the probe when this is in contact with the biological tissue. Generally, the $S_{11}(f)$ measurements can be obtained through a Vector Network Analyzer (VNA) connected to a probe which can be inserted in or in contact with the system under test. For the sake of ensuring in-vivo and non-invasive measurements, a suitable probe configuration is that of a truncated open-ended coaxial probe which when in contact with the tissue sample under test can be sensible to the dielectric variations. To this purpose, it can be exploited the so-called fringing effect associated to a termination flange of the truncated coaxial probe [64]. From the theory [64], to retrieve the $\epsilon^*(f)$ from the corresponding scattering parameter of the MUT, $S_{11,MUT}(f)$ measured in correspondence of the calibration plane, it is essential to know the internal and external fringing capacitances of the

probe. Typically, this technique is implemented in commercially available software and probes, directly provided by the manufacturer: this prevents the implementation on custom probes. However, in view of the specific purposes of the present application, there is the need to use customized probes together with a dedicated customized algorithm. A significant advantage related to the adopted procedure relies on the possibility to completely avoid the quantification of the probe capacitance. Therefore, the specific algorithm, detailed in Section V, can replace the commercial measurement software allowing the possibility of using a customized coaxial probe with comparable accuracy. Finally, a specific procedure [65] was considered to confirm the validity of the considered frequency range for the adopted experimental setup.

IV. PROBE DESIGN AND SIMULATIONS

The aforementioned open-ended coaxial probe, deriving from a “cable truncation” configuration [66], [67], [68] was chosen. However, this basic and general configuration has been customized for the purposes of the proposed work through the use of full-wave simulations in the CST Microwave Studio software, in order to identify the most suitable probe geometry. In particular, for the specific application, the main requirements to be simultaneously optimized in the probe design were: a non-invasiveness and good surface contact with the skin portion under observation, a good spatial resolution and sensitivity in the sensing volume corresponding to the subsurface area of the skin portion, the optimization of the detection performance in the frequency range of interest in terms of discrimination of dielectric differences and, finally, the compatibility with the low-cost miniaturized VNA instrument and the customization possibility. To this purpose and to predict the electromagnetic interaction of the probe on the skin surface, the biological tissue has been modeled through a three-layer structure composed by skin, fat and muscle with the dielectric parameters reported in Table 1. The average thicknesses that were initially considered are 3 mm for skin, 11 mm for fat and 40 mm for muscle. The dielectric parameters considered for the skin are those for the dry condition.

For the sake of optimizing the probe configuration in terms of dielectric sensitivity, some recurrent parametric simulations have been implemented in order to guarantee a good response in the frequency range of interest (which is in the order of few GHz) and to ensure a good spatial resolution in the sensing volume in the subsurface skin region potentially affected by tumoral pathologies. As is well known, the penetration depth of a coaxial probe is proportional to its diameter [69]; hence, as a general requirement, the smaller the diameter, the higher will be the sensitivity related to the skin layer in which the tumour initially originates. As a result, the optimal probe configuration is detailed in Figure 2. In particular, the outer diameter of the inner conductor is 1.25 mm, the inner diameter of the outer conductor is 4.2 mm and the dielectric material between the two conductors is

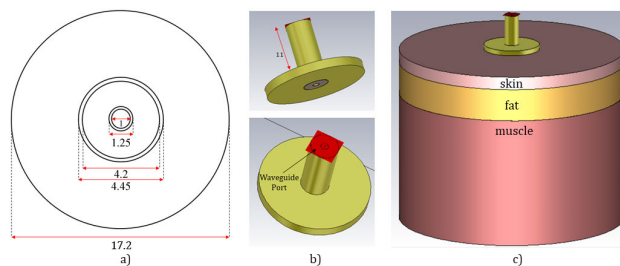


FIGURE 2. Scheme of the simulated system: Bottom view of the probe and geometric dimensions in mm a), Perspective view of the probe b), Probe in contact with the three-layer modeled biological tissue c).

Teflon. The probe, having an external length of 11 mm, is equipped with an external metallic flange (i.e., a ground plane), with a diameter of 17.2 mm, in order to enhance its sensitivity in terms of the fringing field effect, described in Section III. After this preliminary design phase, additional simulations were performed in order to evaluate the response for different thicknesses of the skin layer so as to consider the variability range of different parts of the body [70]. As can be seen in Figure 3, which shows the $S_{11}(f)$ response in function of the skin thickness, the overall behaviour is not substantially influenced by this parameter. As a consequence, the designed probe configuration can be applied on different parts of the body. In addition, it can be stated that the spatial resolution is on the order of about 0.5 mm since, as reported in Figure 3, the system is able to discriminate between 1 mm and 1.5 mm of skin thickness. In particular, this value of spatial resolution is adequate to identify tumor skin lesions at the initial stage. Then, a fixed skin thickness of about 3 mm was considered and additional full-wave simulations were carried out for the fat thickness ranging from 3 mm to 3 cm (which are the typical values of subcutaneous fat for example in the abdomen where it is thickest). As it can be seen from the result reported in Figure 4, the variation in the thickness of the subcutaneous fat layer does not affect significantly the response of the system.

Subsequently, in order to identify the suitable input power level to be used in measurements, two aspects have to be taken into account: safety regulation and human tissue penetration depth. As per the safety issues, in the range between 100 kHz and 10 GHz, current guidelines provide restrictions for electromagnetic fields in terms of the Specific Absorption Rate (SAR). Taking into consideration the International Commission on Non-Ionizing Radiation Protection (ICNIRP) guidelines, in which the SAR limit is 2 W/kg when considering a mass of 10g [71], [72], [73], [74], the SAR value was calculated in CST at a frequency of 0.5 GHz for discrete power levels values up to 1 W. The achieved results are illustrated in Figure 5; it can be seen that values below the limit imposed by safety regulations have been confirmed. As per the EM penetration depth, the goal is to limit it to the skin layer only, so as to allow the detection of possible abnormalities or lesions. In order to optimize the sensitivity

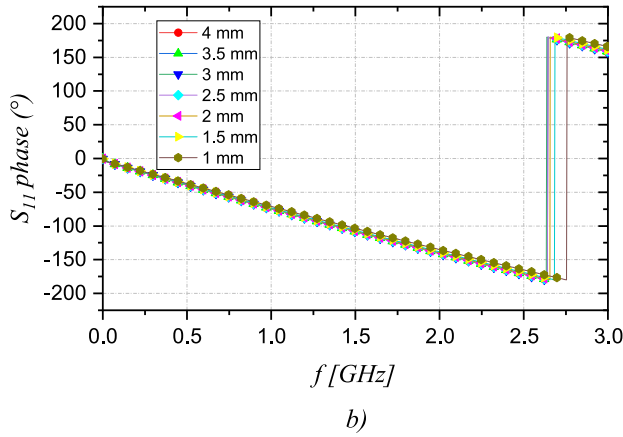
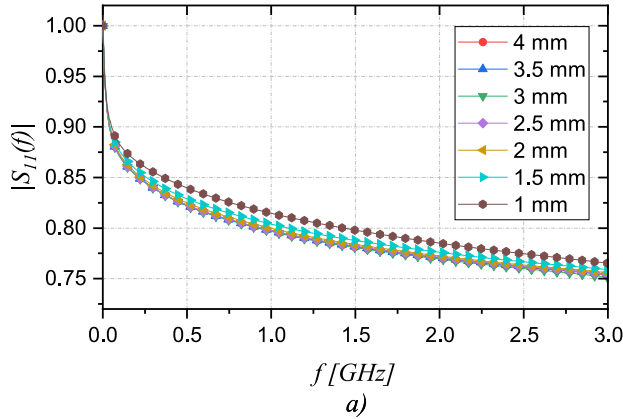


FIGURE 3. Simulated scattering parameter by varying the skin thickness. Magnitude response a), Phase response b).

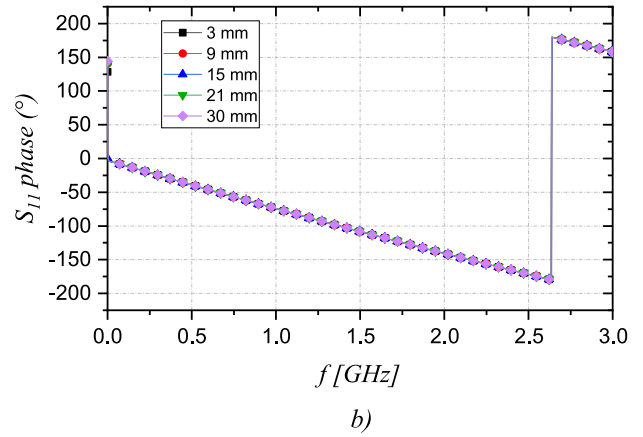
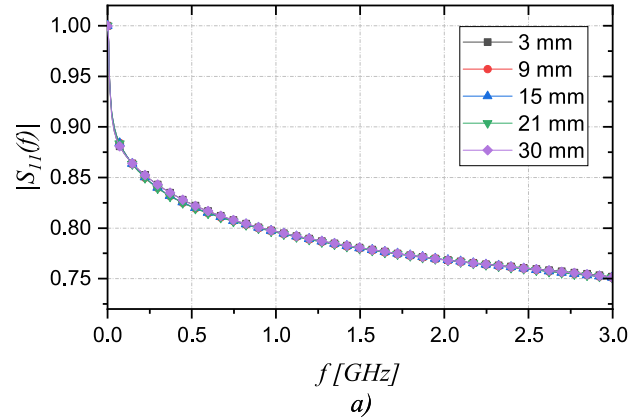


FIGURE 4. Simulated scattering parameter by varying the subcutaneous fat thickness. Magnitude response a), Phase response b).

in the surface portion, an extremely low input power value of -15 dBm (approximately $32 \mu\text{W}$) was chosen, which corresponds to a SAR peak of $4.72 \times 10^{-5} \text{ W/Kg}$. Figure 6 shows the simulation results of the electric field energy density at -15 dBm input power level. As can be seen from the Figure, the field is completely confined within the skin layer and decays very quickly.

V. MATERIALS AND METHODS

The detection procedure involves the initial measurements of the $|S_{11}(f)|$. It is worth mentioning that instruments operating directly in the frequency domain, such as VNAs, compared for example with time domain methods, have the advantage of higher measurement accuracy as calibration procedures that can be implemented to minimize systematic errors. However, the main drawback is that benchtop VNAs, which typically work in a frequency range in the tens of GHz, are very expensive. Recently, low-cost portable VNAs have been made commercially available and they are suitable for measurements over a small range of frequencies. On such basis, in view of the practical application, a miniaturized Vector Network Analyzer (m-VNA) developed by HCXQS (commercially available with the name of nanoVNA) has been chosen. The m-VNA is a compact (dimensions $15 \text{ cm} \times 10 \text{ cm} \times 6 \text{ cm}$),

low-cost (about 100 Euros) VNA with an operating frequency range 50 kHz-3 GHz. For the sake of assessing the metrological performance, a comparative analysis between the m-VNA and a reference benchtop accurate instrument (i.e. VNA R&S ZLV6) was preliminary conducted and reported in Figure 7; as a result, the measurement deviation in terms of root mean square error (RMSE) is 0.0135. After the preliminary validation activity, a specific investigation campaign was conducted involving voluntary people. The experiments were carried out on volunteer subjects who signed informed consent, containing the consent to use and share the anonymized data for scientific publication and the information about the harmlessness of the system. Additionally, the study was conducted according to the guidelines of the Declaration of Helsinki [75] and was approved by the Ethic Committee “Comitato Etico ASL/LE” of the Local Health Authority of Lecce (Italy). The test cases considered in the investigative campaign can be grouped into three major categories: (i) moles that can be regarded as pigmented skin healthy lesions slightly differing from the adjacent normal skin, (ii) malignant and (iii) benign tumours. A group of 11 informed volunteers participated in the research campaign which was conducted with the clinical supervision of the medical personnel who performed the tests and, for each case, diagnosed possible pathologies

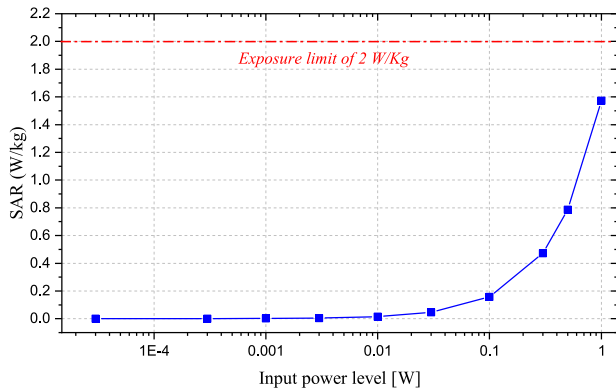


FIGURE 5. Simulation results of SAR values at different input power level.

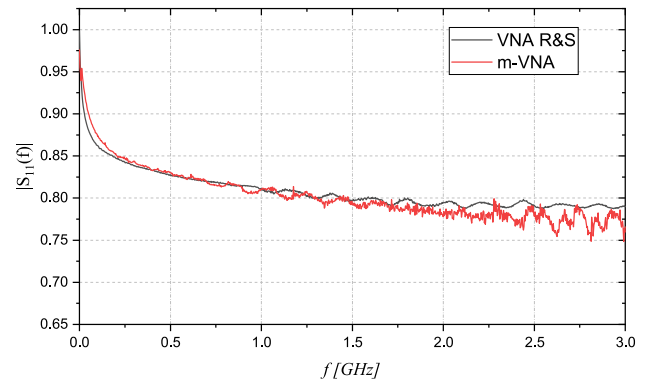


FIGURE 7. Comparison of measurements carried out through the two VNAs.

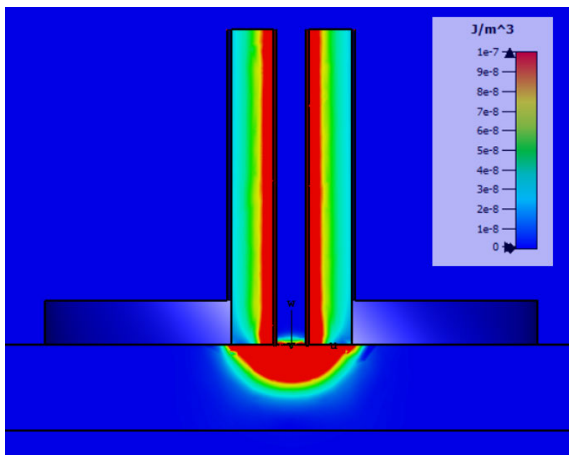


FIGURE 6. Simulation results of E-field density at an input power level of -15 dBm.

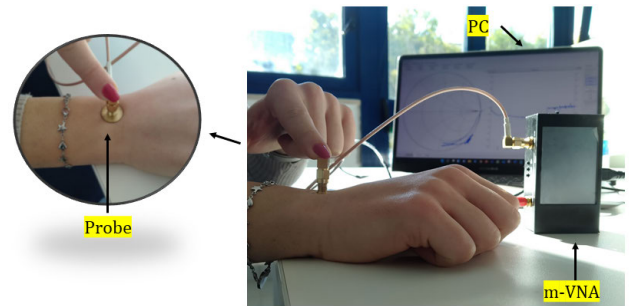


FIGURE 8. Experimental setup highlighting the contact between the skin surface and the probe.

(i.e. both malignant and benign tumours) through the standard so-called ABCDE visual analysis and the epiluminescence. Table 2 summarizes the details of all the analysed cases, also indicating the related body parts and the corresponding dermatological diagnosis. As reported in Table 2, 4 subjects were affected by malignant lesions (two basal cell carcinoma BCC and two epitheliomas), 2 presented benign lesions (keratosis) and, finally, 5 had normal moles.

For each test-case under examination, the adopted in-vivo protocol consisted of a double test; firstly, the suspected area affected by the lesion was investigated and, subsequently, the normal skin area in the proximity of the lesions was also analysed for comparison. Experiments were carried out by connecting the probe to the m-VNA and the raw data was acquired on a PC. Figure 8 shows the used setup highlighting the contact between the skin surface and the probe that, in the current prototypal version of the system, was pressed manually on the skin tissue to ensure a very stable contact. It is worth noting that exerted pressure does not alter or deform human tissue, which is very elastic. For

this reason, the thickness of the tissues remains substantially unchanged.

It should be mentioned that, although the measured response presented a good repeatability, it is envisaged that, in the future, the probe will be inserted in a wearable flexible structure equipped with a miniaturized strength sensor. In order to extrapolate the frequency-dependent dielectric permittivity from the $S_{11}(f)$ measurements, according to the theoretical background described in Section III, a specific algorithm was implemented in LabVIEW, as reported in [76]. More in detail, the extrapolation procedure can be applied for customized coaxial probes, avoiding the complete characterization of the probe capacitance. The procedure, which is described in detail in [76], also implements a specific calibration procedure suitable for the specific probe flange configuration. In particular, this preliminary procedure has to be performed on well-referenced dielectric samples (i.e. ethanol, acetone and propan-2-ol have been chosen) thus allowing compensating for systematic errors [77] and parasitic effect introduced by the setup. For the validation purpose, after the calibration procedure, the customized probe and algorithm were tested and validated considering an additional reference liquid, i.e. methanol (which has known frequency-dependent dielectric characteristics), confirming

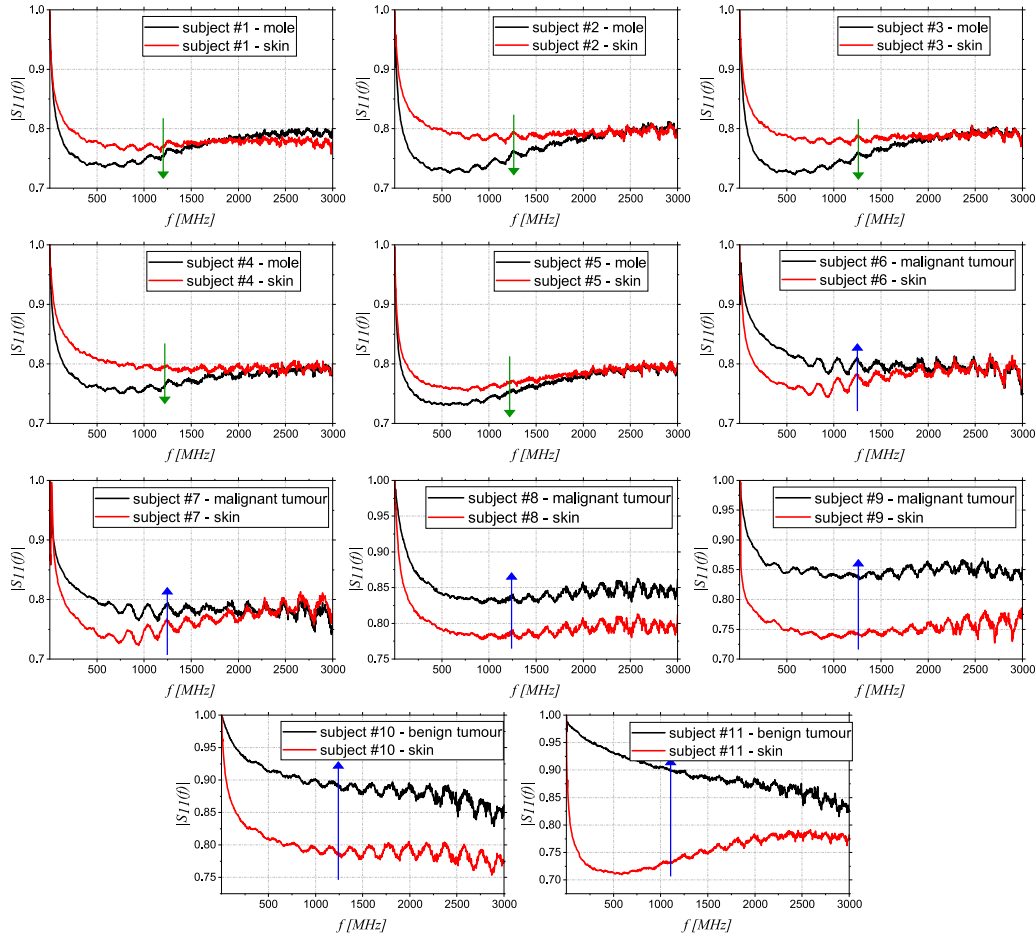


FIGURE 9. Magnitude of the $S_{11}(f)$ measured with the experimental setup on the 11 subjects as categorised: moles, malignant and benign tumours. For each test-case the comparison between lesion and normal skin is reported.

TABLE 2. Characteristics and typologies of the 11 considered test-cases of the voluntary subjects participating in the campaign.

Subject number	Site	Diagnosis	Diameter [mm]
#1	Neck	Mole	6
#2	Cheek	Mole	7
#3	Back	Mole	6
#4	Arm	Mole	5
#5	Thigh	Mole	8
#6	Near ear	Malignant tumour (BCC)	12
#7	Cheek	Malignant tumour (BCC)	16
#8	Nose	Malignant tumour (epithelioma)	10
#9	Cheek	Malignant tumour (epithelioma)	8
#10	Back	Benign tumour (keratosis)	10
#11	Back	Benign tumour (keratosis)	11

a very high accuracy in the extrapolation of the dielectric properties.

VI. EXPERIMENTAL RESULTS

As aforementioned, the experimental measurements were carried out on the 11 volunteer patients, as categorised: moles, malignant tumours and benign tumours. However, the

calibration procedure has been repeated after starting each single measurement session. The measurement results are reported in Figure 9 which shows, for each test-case the comparison between the magnitude of the scattering parameter as acquired from lesions (moles or tumours) and the corresponding normal skin, respectively. As a first observation, it can be noticed that, over the whole considered frequency range, the tumour cases exhibit different values with respect to the moles. The response of moles is systematically lower than that corresponding healthy skin portion, while as for the tumour cases an opposite trend is observed. This preliminary result suggests that the system is capable to discriminate accurately between moles, normal skin and tumours. Additionally, considering the tumours cases, the difference between the responses of benign tumours and healthy skin is more significant. A similar trend was also observed for the phase response of $S_{11}(f)$, not reported for brevity. As described in Section V, from the measured $S_{11}(f)$ data, it is possible to extrapolate the complex permittivity spectrum thus characterizing the specific dielectric signature of the sample. Figure 10 shows the obtained results which refer to the 250 MHz-3 GHz frequency range. As can be easily seen in

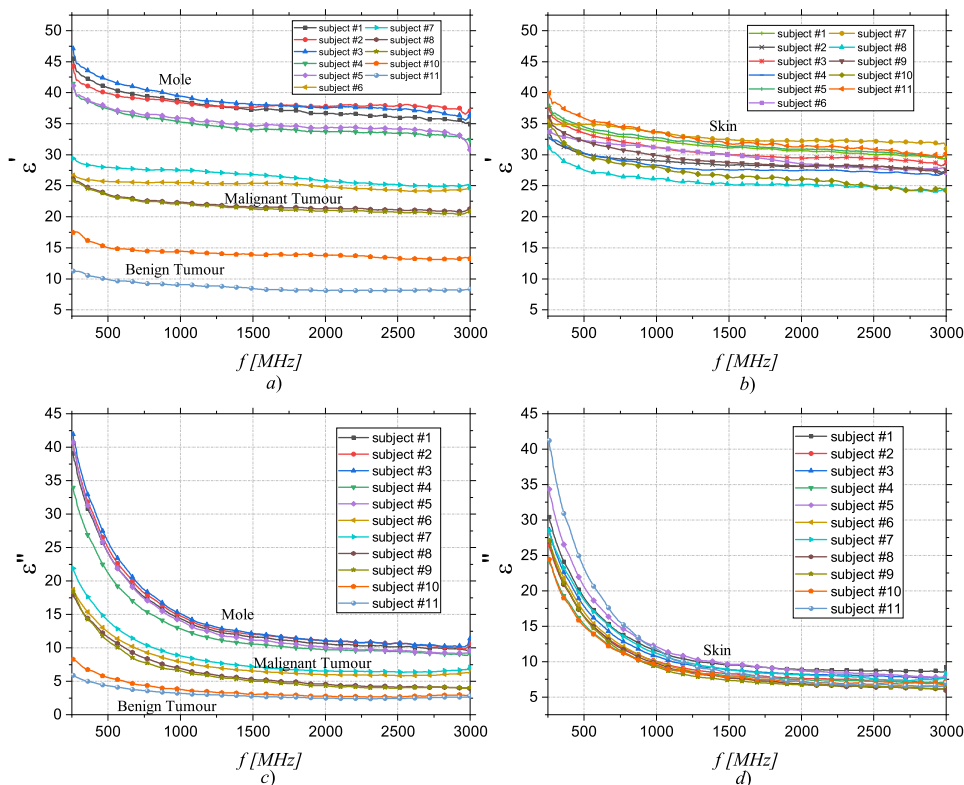


FIGURE 10. Comparative results of the complex permittivity obtained for each considered test-case: Real part of the dielectric permittivity for lesions a) and skin b). Imaginary part of the dielectric permittivity for lesions c) and skin d).

Figure 10, the four tissue categories exhibit different dielectric characteristics. Regarding the skin lesions, it is possible to identify three groups of curves: benign tissues (keratosis) which show the lowest permittivity values, malignant tissues (basal cell carcinoma and epithelioma) which shows the intermediate values and moles which present the highest values of permittivity. The described trend is the same for both the real and the imaginary part of the complex permittivity. The observed trend indicates that the complex permittivity progressively decreases as the tissue degenerates from normal to tumoral condition. In addition, as far as can be observed in this preliminary campaign, the dielectric properties of “normal skin” related to different body areas of different patients highlight “a characteristic dielectric signature” which covers a typical region band presenting a 25% of variation between upper and lower limit. This information, in view of the massive future campaign, could surely be stored in a database and usefully used as a discrimination factor. To further analyse the data, a statistical analysis was performed for facilitating the possible discrimination of different cases and the related classification. Figure 11 shows the mean values (solid lines) and the standard deviation (bars) of the complex permittivity calculated from all the measurements of each of the four tissue groups (moles, healthy skin, malignant tissues and benign tissues).

As a general trend, it is observed that the higher the complex permittivity, the higher the probability that the tissue is not a tumour. Conversely, for dielectric permittivity values lower than those corresponding to the adjacent normal skin, it is necessary a further assessment for discriminating between malignant and benign tumours. However, it must be considered that the measurements carried out in this study are performed completely in vivo [30], preserving the intrinsic characteristics of the tissues, contrarily to what is performed in most of the state of the art where tissue samples taken by biopsy are considered. In addition, to identify similarities among the considered tissues, the Principal Component Analysis (PCA) was carried out on the extrapolated dielectric parameters. The goal is to extract significant information from the data and to present a final classification [78]. The PCA is also useful to identify clusters of elements: the higher is the distance between clusters, the more distinguishable is the data included in the clusters. Figure 12 shows the final result as deriving from the simultaneous processing of both real and imaginary permittivity data. As expected, four main characteristic clusters can be observed. Particularly, considering that moles and healthy skin correspond both to normal conditions, their cumulative cluster area is positioned at the rightmost position of the graph. On the other hand, lesions originating by tumours both malignant and benign

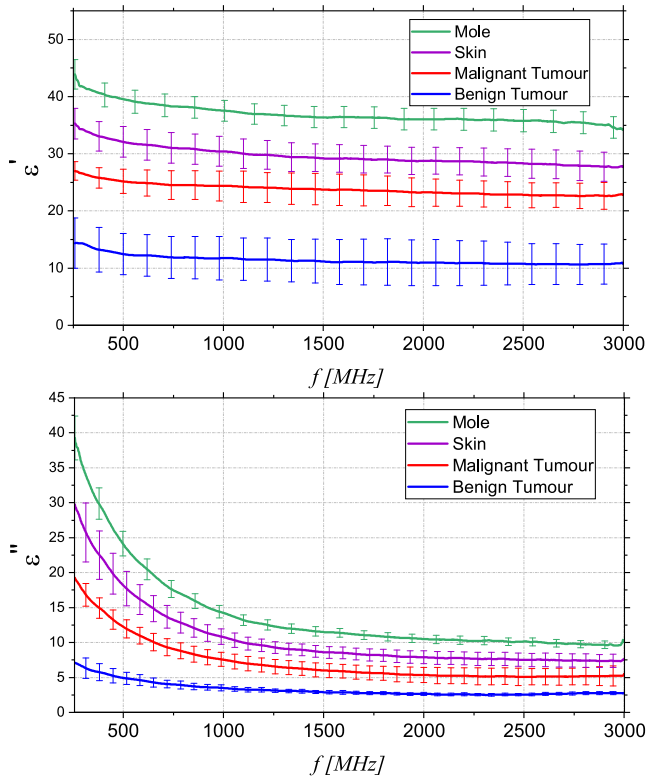


FIGURE 11. Complex permittivity of the five groups of tissues. The lines represent the mean values and the bars the standard deviation. Real part of complex permittivity (ϵ') a) and Imaginary part of complex permittivity (ϵ'') b).

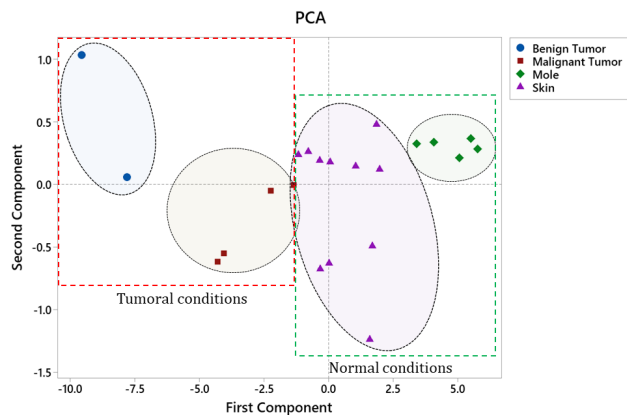


FIGURE 12. Final result of the PCA analysis conducted on the considered test-cases.

appear in the left part of the graph. Although a definitive and high accurate cluster classification would require a bigger dataset, these results indicate that the method is suitable for discriminating among different cases thus anticipating that it is a good candidate for clinical support in early cancer diagnostics.

VII. CONCLUSION

In this paper, a microwave reflectometry-based system for in-vivo skin cancer diagnosis is proposed and experimentally validated. This system potentially offers an attractive solution for non-invasive and in-vivo monitoring to assess early-stage

cancer diagnoses. In this way, it is possible to improve diagnostic accuracy supporting the doctor in making a more objective diagnosis and significantly enhancing the operational aspects of the clinical procedure including the possibility to optimize the requests of biopsies. Furthermore, the system operates in-vivo, it is easy to use and to be transported and it has a very quick response time. The resulting dielectric contrast between healthy and tumoral tissues demonstrates the potential of the system for tissue classification and diagnosis, ensuring simultaneously low cost, compactness and high sensitivity. The observed trend indicates that the complex permittivity progressively decreases as the tissue degenerates from healthy to tumoral condition. Future work will be dedicated to validate and to further test the proposed system on a large-scale campaign and to derive additional important information such as the depth of tumor penetration so as to identify the stage of tumor advancement. Furthermore, in view of the practical application, the system will be improved through the integration of a Bluetooth interface and of a wearable flexible structure entirely realized in bio-materials in order to allow the use also for periodic remote control and clinical monitoring on suspicious or surgically treated areas.

DATA AVAILABILITY

The datasets generated during and/or analysed during the current study are available from Gennaro Maietta on reasonable request sent to gmaietta2001@yahoo.it.

REFERENCES

- [1] The Skin Cancer Foundation. (Jan. 25, 2023). *Official Website*. Accessed: Oct. 5, 2022. [Online]. Available: <https://www.skincancer.org/>
- [2] G. Swann, "The skin is the body's largest organ," *J. Vis. Commun. Med.*, vol. 33, no. 4, pp. 148–149, 2010.
- [3] M. Tampa, S. R. Georgescu, C. I. Mitran, M. I. Mitran, C. Matei, C. Scheau, C. Constantin, and M. Neagu, "Recent advances in signaling pathways comprehension as carcinogenesis triggers in basal cell carcinoma," *J. Clin. Med.*, vol. 9, no. 9, p. 3010, Sep. 2020.
- [4] P. Cohen and A. Calame, "Multiple skin neoplasms at one site (MUSK IN A NEST): A comprehensive review of basal cell carcinoma and benign or malignant 'Collision' tumors at the same cutaneous location," *Clin., Cosmetic Investigational Dermatol.*, vol. 13, pp. 731–741, Nov. 2020.
- [5] A. G. Marzuka and S. E. Book, "Basal cell carcinoma: Pathogenesis, epidemiology, clinical features, diagnosis, histopathology, and management," *Yale J. Biol. Med.*, vol. 88, no. 2, pp. 167–179, 2015.
- [6] M. Alam and D. Ratner, "Cutaneous squamous-cell carcinoma," *New England J. Med.*, vol. 344, no. 13, pp. 975–983, 2001.
- [7] T. M. Johnson, D. E. Rowe, B. R. Nelson, and N. A. Swanson, "Squamous cell carcinoma of the skin (excluding lip and oral mucosa)," *J. Amer. Acad. Dermatol.*, vol. 26, no. 3, pp. 467–484, Mar. 1992.
- [8] C. Massone, A. Di Stefani, and H. P. Soyer, "Dermoscopy for skin cancer detection," *Current Opinion Oncol.*, vol. 17, no. 2, pp. 147–153, Mar. 2005.
- [9] A. Nault, C. Zhang, K. Kim, S. Saha, Y. Bennett, and D. D. Xu, "Biopsy use in skin cancer diagnosis: Comparing dermatology physicians and advanced practice professionals," *JAMA Dermatol.*, vol. 151, no. 8, pp. 899–902, 2015.
- [10] D. MacFarlane and R. Rapini, "Biopsy techniques and interpretation," in *Skin Cancer Management*, D. F. Macfarlane, Eds. New York, NY, USA: Springer, 2009.
- [11] P. Arpaia, E. De Benedetto, and L. Duraccio, "Design, implementation, and metrological characterization of a wearable, integrated AR-BCI hands-free system for health 4.0 monitoring," *Measurement*, vol. 177, Jun. 2021, Art. no. 109280.

- [12] P. Arpaia, E. De Benedetto, C. Dodaro, L. Duraccio, and G. Servillo, "Metrology-based design of a wearable augmented reality system for monitoring patient's vitals in real time," *IEEE Sensors J.*, vol. 21, no. 9, pp. 11176–11183, May 2021.
- [13] J. Baker-Jarvis, M. D. Janezic, P. D. Domich, and R. G. Geyer, "Analysis of an open-ended coaxial probe with lift-off for nondestructive testing," *IEEE Trans. Instrum. Meas.*, vol. 43, no. 5, pp. 711–718, Oct. 1994.
- [14] A. Sarolic, "Open-ended coaxial dielectric probe model for biological tissue sensing depth analysis at 2 GHz," in *Proc. Eur. Microw. Conf. Central Eur. (EuMCE)*, May 2019, pp. 605–608.
- [15] S. A. Komarov, A. S. Komarov, D. G. Barber, M. J. L. Lemes, and S. Rysgaard, "Open-ended coaxial probe technique for dielectric spectroscopy of artificially grown sea ice," *IEEE Trans. Geosci. Remote Sens.*, vol. 54, no. 8, pp. 4941–4951, Aug. 2016.
- [16] D. Berube, F. M. Ghannouchi, and P. Savard, "A comparative study of four open-ended coaxial probe models for permittivity measurements of lossy dielectric/biological materials at microwave frequencies," *IEEE Trans. Microw. Theory Techn.*, vol. 44, no. 10, pp. 1928–1934, Oct. 1996.
- [17] D. L. Gershon, J. P. Calame, Y. Carmel, T. M. Antonsen, and R. M. Hutcheon, "Open-ended coaxial probe for high-temperature and broad-band dielectric measurements," *IEEE Trans. Microw. Theory Techn.*, vol. 47, no. 9, pp. 1640–1648, Sep. 1999.
- [18] S. Sigurdsson, P. A. Philipsen, L. K. Hansen, J. Larsen, M. Gniadecka, and H. C. Wulf, "Detection of skin cancer by classification of Raman spectra," *IEEE Trans. Biomed. Eng.*, vol. 51, no. 10, pp. 1784–1793, Oct. 2004.
- [19] J. Zhang, Y. Fan, Y. Song, and J. Xu, "Accuracy of Raman spectroscopy for differentiating skin cancer from normal tissue," *Medicine*, vol. 97, no. 34, 2018, Art. no. e12022.
- [20] A. Spreinat, G. Selvaggio, L. Erpenbeck, and S. Kruss, "Multispectral near infrared absorption imaging for histology of skin cancer," *J. Biophoton.*, vol. 13, no. 1, Jan. 2020, Art. no. e201960080.
- [21] D. Li, Z. Yang, A. Fu, T. Chen, L. Chen, M. Tang, H. Zhang, N. Mu, S. Wang, G. Liang, and H. Wang, "Detecting melanoma with a terahertz spectroscopy imaging technique," *Spectrochim. Acta A, Mol. Biomol. Spectrosc.*, vol. 234, pp. 1386–1425, Jun. 2020.
- [22] E. Pickwell, A. J. Fitzgerald, P. F. Taday, B. E. Cole, R. J. Pye, T. Ha, M. Pepper, and V. P. Wallace, "Terahertz imaging and spectroscopy of skin cancer," in *Proc. Infr. Millim. Waves, Conf. Dig. Joint 29th Int. Conf. 12th Int. Conf. Terahertz Electron.*, 2004, pp. 821–822.
- [23] L. Ferrante di Ruffano, J. Dinnes, J. J. Deeks, N. Chuchu, S. E. Bayliss, C. Davenport, Y. Takwoingi, K. Godfrey, C. O'Sullivan, R. N. Matin, H. Tehrani, and H. C. Williams, "Optical coherence tomography for diagnosing skin cancer in adults," *Cochrane Database Systematic Rev.*, vol. 12, no. 12, 2018.
- [24] S. Di Meo, A. Cannatà, S. Morganti, G. Matrone, and M. Pasian, "On the dielectric and mechanical characterization of tissue-mimicking breast phantoms," *Phys. Med. Biol.*, vol. 67, no. 15, 2022, Art. no. 155018.
- [25] P. Zakharov, F. Dewaratt, A. Caduff, and M. S. Talary, "The effect of blood content on the optical and dielectric skin properties," *Physiol. Meas.*, vol. 32, no. 1, pp. 131–149, Jan. 2011.
- [26] M. Gniadecka, P. A. Philipsen, S. Wessel, R. Gniadecki, H. C. Wulf, S. Sigurdsson, O. F. Nielsen, D. H. Christensen, J. Herczogova, K. Rossen, H. K. Thomsen, and L. K. Hansen, "Melanoma diagnosis by Raman spectroscopy and neural networks: Structure alterations in proteins and lipids in intact cancer tissue," *J. Investigative Dermatol.*, vol. 122, no. 2, pp. 443–449, Feb. 2004.
- [27] A. Mirbeik-Sabzevari, R. Ashinoff, and N. Tavassolian, "Ultra-wideband millimeter-wave dielectric characteristics of freshly excised normal and malignant human skin tissues," *IEEE Trans. Biomed. Eng.*, vol. 65, no. 6, pp. 1320–1329, Jun. 2018.
- [28] E. Pickwell, A. J. Fitzgerald, B. E. Cole, P. F. Taday, R. J. Pye, T. Ha, M. Pepper, and V. P. Wallace, "Simulating the response of terahertz radiation to basal cell carcinoma using ex vivo spectroscopy measurements," *J. Biomed. Opt.*, vol. 10, no. 6, 2005, Art. no. 064021.
- [29] V. P. Wallace, A. J. Fitzgerald, E. Pickwell, R. J. Pye, P. F. Taday, N. Flanagan, and T. Ha, "Terahertz pulsed spectroscopy of human basal cell carcinoma," *Appl. Spectrosc.*, vol. 60, no. 10, pp. 1127–1133, Oct. 2006.
- [30] H. N. Mayrovitz, S. R. Gildenberg, P. Spagna, L. Killpack, and D. A. Altman, "Characterizing the tissue dielectric constant of skin basal cell cancer lesions," *Skin Res. Technol.*, vol. 24, no. 4, pp. 686–691, Nov. 2018.
- [31] C. Gabriel, *Compilation of the Dielectric Properties of Body Tissues at RF and Microwave Frequencies*. London, U.K.: King's College London, 1996. [Online]. Available: <https://books.google.it/books?id=4MvhMgEACAAJ>
- [32] M. Chren, J. Torres, S. Stuart, D. Bertenthal, R. Labrador, and W. Boscardin, "Recurrence after treatment of nonmelanoma skin cancer: A prospective cohort study," *Arch. Dermatol.*, vol. 147, no. 5, pp. 540–546, 2011.
- [33] F. R. de Grujil, "Skin cancer and solar UV radiation," *Eur. J. Cancer*, vol. 35, no. 14, pp. 2003–2009, Dec. 1999.
- [34] A. Halpern and J. Altman, "Genetic predisposition to skin cancer," *Current Opinion Oncol.*, vol. 11, no. 2, pp. 132–138, 1999.
- [35] K. Tsai and H. Tsao, "The genetics of skin cancer," *Amer. J. Med. Genet. C, Seminars Med. Genet.*, vol. 131, no. 1, pp. 82–92, 2004.
- [36] M. M. L. Brown, C. A. B. Sharpe, D. S. Macmillan, and V. J. McGovern, "Genetic predisposition to melanoma and other skin cancers in Australians," *Med. J. Aust.*, vol. 1, no. 16, pp. 852–853, Apr. 1971.
- [37] G. Danaei, S. Vander Hoorn, A. Lopez, C. Murray, and M. Ezzati, "Causes of cancer in the world: Comparative risk assessment of nine behavioural and environmental risk factors," *Lancet*, vol. 366, no. 9499, pp. 1784–1793, 2005.
- [38] M. R. Gerstenblith, J. Shi, and M. T. Landi, "Genome-wide association studies of pigmentation and skin cancer: A review and meta-analysis: Review of skin cancer and pigmentation GWAS," *Pigment Cell Melanoma Res.*, vol. 23, no. 5, pp. 587–606, Oct. 2010.
- [39] F. Urbach, "Geographic distribution of skin cancer," *J. Surgical Oncol.*, vol. 3, no. 3, pp. 219–234, 1971.
- [40] H. Auerbach, "Geographic variation in incidence of skin cancer in the United States," *Public Health Rep.*, vol. 76, no. 4, pp. 345–348, 1961.
- [41] R. S. Stern, "The mysteries of geographic variability in nonmelanoma skin cancer incidence," *Arch. Dermatol.*, vol. 135, no. 7, pp. 843–844, Jul. 1999.
- [42] S. Rangwala and K. Y. Tsai, "Roles of the immune system in skin cancer," *Brit. J. Dermatol.*, vol. 165, no. 5, pp. 953–965, Nov. 2011.
- [43] C. A. Harwood and C. M. Proby, "Human papillomaviruses and non-melanoma skin cancer," *Current Opinion Infectious Diseases*, vol. 15, no. 2, pp. 101–114, 2002.
- [44] I. Nindl and F. Rösl, "Molecular concepts of virus infections causing skin cancer in organ transplant recipients," *Amer. J. Transplantation*, vol. 8, no. 11, pp. 2199–2204, Nov. 2008.
- [45] D. Rigel, R. Friedman, A. Kopf, and D. Polsky, "ABCDE—An evolving concept in the early detection of melanoma," *Arch. Dermatol.*, vol. 141, no. 8, pp. 1032–1034, 2005.
- [46] J. K. Robinson and S. Ortiz, "Use of photographs illustrating ABCDE criteria in skin self-examination," *Arch. Dermatol.*, vol. 145, no. 3, pp. 332–333, Mar. 2009.
- [47] N. Giaquinto, G. M. D'Aucelli, E. De Benedetto, G. Cannazza, A. Cataldo, E. Piuze, and A. Masciullo, "Criteria for automated estimation of time of flight in TDR analysis," *IEEE Trans. Instrum. Meas.*, vol. 65, no. 5, pp. 1215–1224, May 2016.
- [48] A. Cataldo, E. De Benedetto, G. Cannazza, E. Piuze, and N. Giaquinto, "Embedded TDR wire-like sensing elements for monitoring applications," *Measurement*, vol. 68, pp. 236–245, May 2015.
- [49] A. Cataldo, E. De Benedetto, G. Cannazza, E. Piuze, and E. Pittella, "TDR-based measurements of water content in construction materials for in-the-field use and calibration," *IEEE Trans. Instrum. Meas.*, vol. 67, no. 5, pp. 1230–1237, May 2018.
- [50] A. Cataldo, G. Monti, E. De Benedetto, G. Cannazza, L. Tarricone, and L. Catarinucci, "Assessment of a TD-based method for characterization of antennas," *IEEE Trans. Instrum. Meas.*, vol. 58, no. 5, pp. 1412–1419, May 2008.
- [51] E. Piuze, G. Cannazza, A. Cataldo, E. De Benedetto, L. De Giorgi, F. Frezza, G. Leucci, S. Pisa, E. Pittella, S. Prontera, and F. Timpani, "A comparative assessment of microwave-based methods for moisture content characterization in stone materials," *Measurement*, vol. 114, pp. 493–500, Jan. 2018.
- [52] A. Cataldo, R. Schiavoni, A. Masciullo, G. Cannazza, F. Micelli, and E. De Benedetto, "Combined punctual and diffused monitoring of concrete structures based on dielectric measurements," *Sensors*, vol. 21, no. 14, p. 4872, Jul. 2021.
- [53] E. Pittella, R. Schiavoni, G. Monti, A. Masciullo, M. Scarpetta, A. Cataldo, and E. Piuze, "Split ring resonator network and diffused sensing element embedded in a concrete beam for structural health monitoring," *Sensors*, vol. 22, no. 17, p. 6398, Aug. 2022.

- [54] A. Cataldo, G. Cannazza, E. De Benedetto, and N. Giaquinto, "Experimental validation of a TDR-based system for measuring leak distances in buried metal pipes," *Prog. Electromagn. Res.*, vol. 132, pp. 71–90, 2012.
- [55] A. Cataldo, E. De Benedetto, G. Cannazza, G. Monti, and E. Piuze, "TDR-based monitoring of rising damp through the embedding of wire-like sensing elements in building structures," *Measurement*, vol. 98, pp. 355–360, Feb. 2017.
- [56] R. Schiavoni, G. Monti, E. Piuze, L. Tarricone, A. Tedesco, E. De Benedetto, and A. Cataldo, "Feasibility of a wearable reflectometric system for sensing skin hydration," *Sensors*, vol. 20, no. 10, p. 2833, May 2020.
- [57] A. Cataldo, E. De Benedetto, R. Schiavoni, G. Monti, A. Tedesco, A. Masciullo, E. Piuze, and L. Tarricone, "Portable microwave reflectometry system for skin sensing," *IEEE Trans. Instrum. Meas.*, vol. 71, pp. 1–8, 2022.
- [58] R. Schiavoni, G. Monti, A. Tedesco, L. Tarricone, E. Piuze, E. De Benedetto, A. Masciullo, and A. Cataldo, "Microwave wearable system for sensing skin hydration," in *Proc. IEEE Int. Instrum. Meas. Technol. Conf. (I2MTC)*, May 2021, pp. 1–6.
- [59] A. Cataldo, E. De Benedetto, L. Angrisani, G. Cannazza, and E. Piuze, "A microwave measuring system for detecting and localizing anomalies in metallic pipelines," *IEEE Trans. Instrum. Meas.*, vol. 70, pp. 1–11, 2021.
- [60] A. Cataldo, E. De Benedetto, R. Schiavoni, A. Tedesco, A. Masciullo, and G. Cannazza, "Microwave reflectometric systems and monitoring apparatus for diffused-sensing applications," *ACTA IMEKO*, vol. 10, no. 3, p. 202, Sep. 2021.
- [61] P. Mehta, K. Chand, D. Narayanswamy, D. G. Beetner, R. Zoughi, and W. V. Stoecker, "Microwave reflectometry as a novel diagnostic tool for detection of skin cancers," *IEEE Trans. Instrum. Meas.*, vol. 55, no. 4, pp. 1309–1316, Aug. 2006.
- [62] M. Gniadecka, O. F. Nielsen, and H. C. Wulf, "Water content and structure in malignant and benign skin tumours," *J. Mol. Struct.*, vols. 661–662, pp. 405–410, Dec. 2003.
- [63] C. Gabriel, S. Gabriel, and E. Corthout, "The dielectric properties of biological tissues: I. literature survey," *Phys. Med. Biol.*, vol. 41, no. 11, pp. 2231–2249, Nov. 1996.
- [64] Y. Wei and S. Sridhar, "Radiation-corrected open-ended coax line technique for dielectric measurements of liquids up to 20 GHz," *IEEE Trans. Microw. Theory Techn.*, vol. 39, no. 3, pp. 526–531, Mar. 1991.
- [65] W. J. Ellison and J.-M. Moreau, "Open-ended coaxial probe: Model limitations," *IEEE Trans. Instrum. Meas.*, vol. 57, no. 9, pp. 1984–1991, Sep. 2008.
- [66] E. Piuze, E. Pittella, S. Pisa, A. Cataldo, E. De Benedetto, and G. Cannazza, "Microwave reflectometric methodologies for water content estimation in stone-made cultural heritage materials," *Measurement*, vol. 118, pp. 275–281, Mar. 2018.
- [67] A. La Gioia, E. Porter, I. Merunka, A. Shahzad, S. Salahuddin, M. Jones, and M. O'Halloran, "Open-ended coaxial probe technique for dielectric measurement of biological tissues: Challenges and common practices," *Diagnostics*, vol. 8, no. 2, p. 40, Jun. 2018.
- [68] J. S. Bobowski and T. Johnson, "Permittivity measurements of biological samples by an open-ended coaxial line," *Prog. Electromagn. Res.*, vol. 40, pp. 159–183, 2012.
- [69] P. M. Meaney, A. P. Gregory, J. Seppälä, and T. Lahtinen, "Open-ended coaxial dielectric probe effective penetration depth determination," *IEEE Trans. Microw. Theory Techn.*, vol. 64, no. 3, pp. 915–923, Mar. 2016.
- [70] J. Sandby-Møller, T. Poulsen, and H. C. Wulf, "Epidermal thickness at different body sites: Relationship to age, gender, pigmentation, blood content, skin type and smoking habits," *Acta Dermato Venereol.*, vol. 83, no. 6, pp. 410–413, 2003, doi: [10.1080/00015550310015419](https://doi.org/10.1080/00015550310015419).
- [71] *IEEE Standard for Safety Levels With Respect to Human Exposure to Radiofrequency Electromagnetic Fields, 3 KHz to 300 GHz*, IEEE Standard C95.1, 2005.
- [72] The International Commission on Non-Ionizing Radiation Protection, "Guidelines for limiting exposure to time-varying electric, magnetic, and electromagnetic fields (up to 300 GHz)," *Health Phys.*, vol. 74, no. 4, pp. 494–522, Apr. 1998.
- [73] *IEEE Recommended Practice for Measurements and Computations of Radio Frequency Electromagnetic Fields With Respect to Human Exposure to Such Fields, 100 KHz-300 GHz*, IEEE Standard C95.3-1991), IEEE Standard C95.3-2002, 2002.
- [74] Federal Communications Commission Office of Engineering Technology OET Bulletin 65, *Evaluating Compliance With FCC Guidelines for Human Exposure to Radiofrequency Electromagnetic Fields*, 1997.
- [75] World Medical Association, "World Medical Association Declaration of Helsinki: Ethical principles for medical research involving human subjects," *JAMA*, vol. 310, no. 20, pp. 2191–2194, 2013.
- [76] E. Piuze, C. Merla, G. Cannazza, A. Zambotti, F. Apollonio, A. Cataldo, P. D'Atanasio, E. De Benedetto, and M. Liberti, "A comparative analysis between customized and commercial systems for complex permittivity measurements on liquid samples at microwave frequencies," *IEEE Trans. Instrum. Meas.*, vol. 62, no. 5, pp. 1034–1046, May 2013.
- [77] F. Attivissimo, A. Cataldo, L. Fabbiano, and N. Giaquinto, "Systematic errors and measurement uncertainty: An experimental approach," *Measurement*, vol. 44, no. 9, pp. 1781–1789, Nov. 2011.
- [78] I. Jolliffe, "Principal component analysis, in *Encyclopedia of Statistics in Behavioral Science*, B. S. Everitt and D. C. Howell, Eds. New York, NY, USA: Wiley, 2010, pp. 1580–1584.

RAISSA SCHIAVONI received the M.S. degree in communication engineering and electronic technologies from the University of Salento, Italy, in 2020, where she is currently pursuing the Ph.D. degree in complex systems engineering. Her research interests include microwave reflectometry systems for monitoring applications.

GENNARO MAIETTA received the M.S. degree in medicine and surgery from the University of Florence, Florence, Italy, in 1981. Subsequently, he completed his specialty training in immunology and allergology, in 1984, and dermatology and sexually transmitted diseases, in 1988.

ELISABETTA FILIERI received the M.S. degree in medicine and surgery from Ferrara University, in 2009. Her M.S. thesis was titled "Hairy Cell Leukemia." Subsequently, she moved to Modena University, where she completed speciality in medical oncology, in 2015. She works both in clinical and research field, mainly on breast and gynecological cancers.

ANTONIO MASCIULLO received the M.S. degree in electronic engineering from the Politecnico di Bari, Bari, Italy, in 1995, and the Ph.D. degree in information engineering from the University of Salento, Lecce, Italy, in 2015. Since 2003, he has been with the Department of Innovation Engineering, University of Salento, where he is currently a Laboratory Technician of Telecommunications, Automatic Control, and Electronic Measurement Laboratories.

ANDREA CATALDO (Senior Member, IEEE) is currently an Associate Professor of electric and electronic measurements with the Department of Engineering for Innovation of University of Salento, LECCE, Italy. He is also the Founder of University spin-off company MoniteTech. He is the inventor of four patents. He has coauthored more than 200 publications and three books. He has coordinated several scientific and industrial projects. His research interests include reflectometry and microwave measurement techniques, uncertainty evaluation, characterization and optimization of sensors, and biomedical sensors. He is a member of the IEEE Instrumentation and Measurement (I&M) Society and an editorial member of different journals.

• • •

Open Access funding provided by 'Università del Salento' within the CRUI CARE Agreement